International Journal of Pavement Engineering

ISSN: (Print) (Online) Journal homepage: https://www.tandfonline.com/loi/gpav20

Mix design and laboratory characterisation of rubberised mixture used as damping layer in pavements

Jiandong Huang, Pietro Leandri, Giacomo Cuciniello & Massimo Losa

To cite this article: Jiandong Huang, Pietro Leandri, Giacomo Cuciniello & Massimo Losa (2022) Mix design and laboratory characterisation of rubberised mixture used as damping layer in pavements, International Journal of Pavement Engineering, 23:8, 2746-2760, DOI: 10.1080/10298436.2020.1869975

To link to this article: https://doi.org/10.1080/10298436.2020.1869975

INTERNATIONAL JOURNAL OF PAVEMENT ENGINEERING
2022, VOL. 23, NO. 8, 2746–2760
https://doi.org/10.1080/10298436.2020.1869975

Mix design and laboratory characterisation of rubberised mixture used as damping layer in pavements

Jiandong Huang, Pietro Leandri, Giacomo Cuciniello and Massimo Losa

Department of Civil and Industrial Engineering, University of Pisa, Pisa, Italy

ABSTRACT

Road authorities are challenged by traffic-induced vibrations due to their detrimental effects on humans and to the damage of buildings and structures. For this reason, asphalt mixtures designed as damping layer are investigated to resist vibration and noise caused by traffic loads, while a reliable design method to optimise for the mixes needs to be developed and their damping and mechanical properties require corresponding evaluation. In this work, a novel mix-design method special for the damping layer is proposed. Two rubberised asphalt mixtures were designed by optimising their damping properties and their volumetrics were adjusted to accommodate a high content of rubberised bitumen. Tensile strength, rutting resistance, stiffness, loss factor, phase angle and damping ratio were measured to evaluate their mechanical and functional potential as thin damping interlayer in road pavements. Results show that the designed mixes have higher damping capacity than traditional rubberised asphalt mixes. Aside from this, the mixes appear to be rut resistant and show sufficient levels of tensile strength and resistance to water damage.

ARTICLE HISTORY
Received 16 June 2020
Accepted 23 December 2020

KEYWORDS
Damping; vibration; rubberised asphalt mixes; dynamic modulus; phase angle; rutting

1. Introduction

Vibrations induced by road traffic is of concern worldwide. The vibratory mechanism affects the quality of life of people daily and nightly hours. Such annoyance shall not be underestimated since it seems to be the cause of stress-related human diseases (Houghton 1994).

Besides the effects on humans, vibrations affect the integrity of historical buildings and can undermine the stability of sensitive buildings as hospitals, scientific research labs, and high-tech industries (Hunaidi and Tremblay 1997, Clemente and Rinaldis 1998, Hao *et al.* 2001, Ouis 2001, Ju and Ni 2007, Browne *et al.* 2012). Furthermore, road vibrations cause traffic noise in the range of frequencies below 1000 Hz (Sandberg 1999).

Considering the severity of this problem, preventive strategies are under investigation. Examples of these strategies are traffic restrictions (volumes and speed), in-ground barriers, and isolating systems (Hunaidi *et al.* 2000). In the field of pavement engineering, the so-called anti-vibration paving technology is under investigation to avoid the generation of excessive vibration with the approach of the damping layer (Simone *et al.* 2008, Cantisani *et al.* 2013, Venturini *et al.* 2016, Huang *et al.* 2018). To preserve an ancient building (the Villa Farnesina, Roma) against traffic-induced vibrations, an anti-vibration system composed of a concrete grid supported by rubber pads, was developed under the near Lungo Tevere road, reducing the acceleration values of about 80% according to the obtained results. Similar solutions have also been used for new constructions in Piazzetta S. Paolo, Milan, and Via Parigi, Roma (Clemente and Rinaldis 1998). The anti-vibration pavement has also been developed by Dondi and Simone (2005) and Grandi (2008) with a lower-stiffness vibration-absorbing layer which did not reduce the stiffness of the whole pavement systems. Such anti-vibration pavement has been proved to increase the elastic absorption capacity of the vibrations caused by the surface irregularities near the source. Based on the optimised surface texture as well as the improvement of the vibration absorbing, another type of anti-vibration pavement was constructed for the Municipality of Novara (Venturini *et al.* 2016). The verification is conducted by the vibration comparison of the anti-vibration pavement and one reference, showing the anti-vibration level reached. However, it should be noted that the previous design of the damping layer is often an empirical design, that is, the lack of determination of the design criteria for the asphalt mixture used in the damping layer. In addition, the previous research lacks the analysis of the mechanical properties and damping performance of the designed damping layer on a laboratory scale. As far as such design criteria concerned, the damping properties of asphalt mixes are optimised to reduce vibrations (Hanazato *et al.* 1991, County 1999). The relations between the composition of asphalt mixes, their damping properties, and effects on traffic-induced vibrations have been investigated for more than two decades (Cho *et al.* 1998, Zhu and Carlson 2001, Zhong *et al.* 2002, Paje *et al.* 2010, Schubert *et al.* 2010, Wang and Höeg 2010, Wang *et al.* 2011, Di Mino *et al.* 2012, Maggiore *et al.* 2012). Findings have highlighted that the use of crumb rubber (CR) from the end of life tires (ELT) in asphalt mixes improves their damping response. Wang *et al.* (2011) investigated the production of damping materials by using rubberised mixes as a replacement of the basalt in the foundation layer. The resonance column was used to measure the stiffness and damping ratio of rubber-modified asphalt mixes

CONTACT Giacomo Cuciniello giacomo.cuciniello83@dc.unipi.it

prepared with different rubber contents. Findings highlighted that rubberised-mixes could be used in the foundation of the railway track bed for high-speed trains to reduce vibration due to their damping properties.

Biligiri (2013) used the phase angle as an indicator of the noise-damping properties of asphalt mixes in the field. The authors highlighted that rubberised mixes with high binder content, high porosity, and rubber inclusions, show improved damping and acoustic performances.

In 2018, Huang and co-workers presented a theoretical model to predict the damping ratio of a road pavement specifically designed to mitigating traffic-induced vibrations. The pavement was composed of a damping layer at the interface between the binder and the base layer. Based on model results, to be effective in mitigating vibrations, they defined some target values of the material damping composing the interlayer. Specifically, in the modelled pavement structure, to achieve a decrease of vibration accelerations at the soil surface away from the wheel track, they calculated at least a double value of the damping ratio of the interlayer compared to that of a conventional mix.

However, although rubberised asphalt mixes have resulted in being effective in absorbing vibrations when adopted in road pavements and track beds, a reliable design method to optimise their damping and mechanical properties needs to be developed.

From the functional characteristics of vibration reduction, damping is intended as the capacity of (viscoelastic) materials to dissipate mechanical energy (Zinoviev and Ermakov 1994, Inaudi and Kelly 1995, Feriani and Perotti 1996, Michaels 2008, Phillips and Hashash 2008). A critical distinction is made between damping of a composite structure, and damping as a material property (i.e. intrinsic damping). The first entails hysteresis, friction at joints, and other phenomena occurring in the structure that causes energy dissipation. Friction between two surfaces is a clear example of this. The damping of structures depends on multiple phenomena that affect the overall dynamic response (Bergman and Hannibal 1976). For this reason, this type of damping is not modelled at the constitutive level of the materials that compose the structure. On the other hand, the intrinsic damping is a material property, and it is typically modelled considering constitutive relations and rheological properties of materials as road bitumens (Dos Reis 1999, Wang *et al.* 2011, Gudmarsson *et al.* 2013).

According to many authors (Lazan 1968, Nashif *et al.* 1985), the loss factor (η) is the viscoelastic function most representative of intrinsic damping (Equation (1)),

$$\eta = \tan \delta \tag{1}$$

where δ is the phase angle.

The loss factor can be successfully applied to nonlinear systems, used in material testing or in evaluating composite structures. It measures energy dissipation irrespective of the physical mechanisms involved. The original definition of η refers to the time-lag between stress and strain under sinusoidal cyclic loadings, and it is a measure of the dissipative mechanisms in the materials. The higher is the loss factor, the more the material dissipates energy under loading (Lakes 2009).

Asphalt mixes are composite materials and cannot be truly defined as structures. In a single degree of freedom vibrating system, three parameters, namely, mass, viscous damping coefficient, and stiffness characterise the vibration of a structural element. This analogy also applies to the transmission of vibrations through the pavement material. Therefore, the damping response can be characterised by mass and stiffness of the material along with its inherent viscous damping characteristics. For simple harmonic excitation (e.g. tire rolling on a pavement surface) in a complex modulus material (such as asphalt mixes), studies have shown that phase angle δ, and damping ratio ζ can be related by Equation (2) (Biligiri 2013).

$$\zeta = \frac{1}{2} \tan \delta \tag{2}$$

Asphalt mixes are designed to be rutting and fatigue cracking resistant (Bahia *et al.* 2001, Witczak 2002). These requirements have been challenged by the viscoelastic nature of bitumens that causes energy dissipation and consequent failure. Considering this, increasing the damping properties of mixes could be seen as something against the adopted design criteria. Therefore, mixes for damping layers shall be designed to mitigate vibrations under the constraints of adequate durability.

The optimisation of damping properties of pavements is novel if compared with other traditional criteria (Kuo and Tsai 2014). Therefore, if rutting resistance and fatigue cracking resistance can be balanced, the effects of optimised damping properties on them require still investigation. Therefore, there is a need for more advanced analytical and experimental tools to enable designers to account for damping properties in pavement materials.

2. Research significance and objectives

The significance of this study is to propose a design method for asphalt mixtures suitable for damping layers, and to verify its feasibility through the characterisation of laboratory tests. Specifically, it aims at the design of two asphalt mixes prepared with high contents of wet-rubberised binder (Asphalt Rubber – AR), to be used in the construction of a damping layer in road pavements. The designed damping mixtures are to evaluate and understand the mechanical and functional (damping) properties to verify their practicality in construction. During such process, the study also aims to propose and modify the suitable experimental methods or guidelines for this kind of special asphalt mixture.

3. Materials and methods

3.1. Materials

3.1.1. Rubberised binder

The rubberised binder was plant-produced according to the ASTM D6114-97 (2002) by a local manufacturer in Tuscany. A penetration (Pen) 50–70 was used as base bitumen with 20% of crumb rubber derived from the mechanical grinding

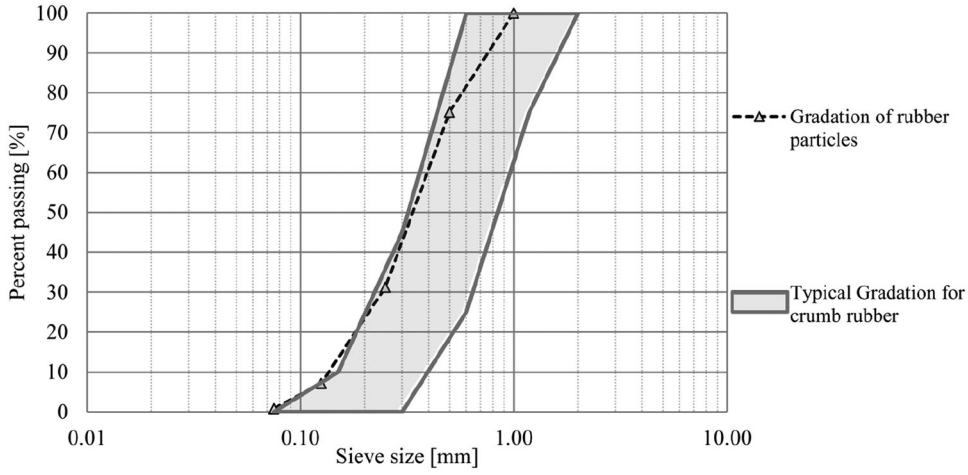

Figure 1. Gradation of rubber particles.

at room temperature of waste scrape tires. The gradation of the crumb rubber is given in Figure 1.

3.1.2. Aggregates

The dry mix was constituted of coarse basalt aggregates, natural sand, and mineral filler. The physical properties of the aggregates are given in Table 1.

3.2. Research methods

The research methodology is presented by the work chart in Figure 2. A conventional open-graded (OG) asphalt mixture was used as a starting point to design the damping asphalt mixture based on the design criteria proposed in the present study. At the same time, it was employed as the control mixture to compare tensile strength, water sensitivity, dynamic modulus, phase angle, and rutting resistance with the designed damping mixture. Besides mechanical properties, damping properties were evaluated through the measurement of the damping ratio and loss factor.

3.3. Design of mixes

Increasing damping properties of asphalt mixes requires the use of higher volumes of (rubberised) binder compared to hot mix asphalt prepared with traditional Crumb Rubber Modified binder. For this reason, the mix design has the scope to accommodate a sufficient volume of rubberised binder to increase damping, while maintaining adequate stability and resistance.

The use of an open-graded (OG) mix allows a large volume of voids in mineral aggregates (VMA), and the aggregate interlock is provided by crushed angular tough basalt aggregates. Traditionally, this mix is designed to achieve a volume of air voids in compacted mixes between 20 and 25% to provide water drainage and noise absorption. In the damping layers, the large VMA available needs to be filled with rubberised asphalt to increase the volume of effective bitumen (V_{be} – bitumen not absorbed in mineral aggregates). The latter is representative of the mortar (bitumen + filler) film thickness that coats the aggregates (coarse and fine) (Underwood and Kim 2011).

Higher values of VMA and V_{be} are likely to increase the durability of mixes providing a higher fatigue resistance and a lower oxidative susceptibility (Kandhal and Chakraborty 1996). However, the excessive binder content could affect the stability of the mixes at high temperatures worsening their rutting resistance (Christensen and Bonaquist 2005). The large film thickness of mortar coating the aggregates could reduce the grain-to-grain contact in the aggregates skeleton reducing the stability of the mixture. In the case of mixes for damping layers, the scope is to maximise damping; therefore, the volume of bitumen used is not representative of traditional mixes. However, the optimisation of the damping properties cannot affect the rutting resistance of mixes. For this reason, the primary criterion behind their design is to increase damping while maintaining stability and rutting resistance. To do so, it is necessary to stiffen the mastic coating the aggregates by increasing the volume fraction of filler. In other words, the amount of binder shall be increased contextually with the amount of filler.

Table 1. Physical properties of aggregates (EN 1097-6/7).

Properties	Basalt	Sand	Mineral Filler
Bulk Specific Gravity (G_{sb}) [kg/m^3]	2.753	2.629	2.710
Water Absorption [%]	1.39	0.86	-

3.3.1. Reference mixture

An Open-Graded (0–8 mm) mixture was selected as the reference mixture (Mix_{ref}). This mix design was optimised in a previous project to achieve the desired functional and mechanical performances (Losa and Leandri 2012). The mixture was compacted in the Superpave Gyratory Compactor (SGC) according to EN 12697-31 (2019) and using mixing and compaction temperatures equal to 180°C under the recommendation of the bitumen supplier. The mix was compacted at 130 gyrations. The gradation of Mix_{ref} is given in Figure 3.

The volumetric properties are given in Table 2.

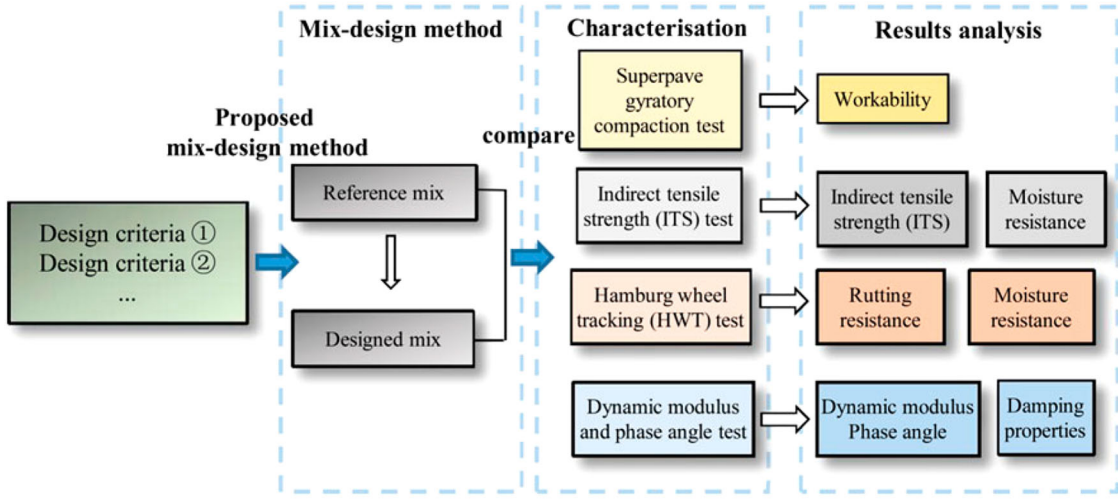

Figure 2. Flow chart of the experiment.

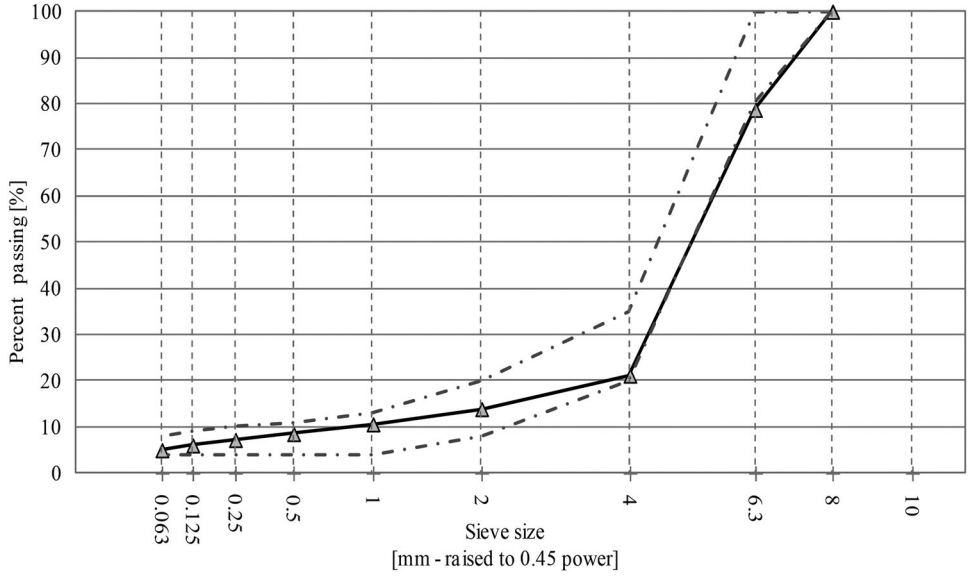

Figure 3. Gradation of Reference Mixture (Mix_{ref}).

The mixes for damping layers were designed starting from this mix.

3.3.2. Mixes for damping layer (Mix 1 and Mix 2)

The mixes were prepared in the SGC at the same mixing and compaction temperatures of the reference mixture. The gradations and volumetrics of the mixes for damping layers are shown respectively in Figure 4 and Table 3.

Volumetrics for mix design were calculated on compacted 100 mm diameter mixes (Table 3).

The two mixes include a higher bitumen content compared to the reference mixture (+ 9.8% and +15.0% by weight of aggregates for Mix 1 and Mix2 respectively). The amount of binder in the mix has been increased as long with the amount of filler. Table 3 shows that Mix 1 and Mix 2 have a higher amount of filler compared to the reference mixture (Table 2) (+9.9% and +15.0% respectively). It has to be noted that the filler and binder have been increased by maintaining the same D/P proportion (~1) of Mix_{ref}. This aspect indicates that the amount of binder has been maximised by maintaining the same volume fraction of filler in the mastic. For this reason, the mastics in the three mixes were expected to have similar levels of stiffness, preventing them from losing stability and from becoming rutting susceptible due to the high binder content.

Table 2. Volumetric properties (by weight and by volume) of reference mixture (EN 12697 – Part 5, 6) (2012).

Composition	Agg. [%]	Filler [%]	Binder [%]	N_{max} [gg]	AV[%]	VMA [%]	VFA [%]	D/P [1]
Weight (W)	95.2	4.8	5.0	130	-	35.2	23.8	0.96
Volume (V)	61.7	3.1	8.4		26.8			

(N_{des} – Design gyrations number of SGC; AV – Air Voids; VMA – Voids in Mineral Aggregates; VFA – Voids filled with Asphalt; DP – Dust to binder ratio).

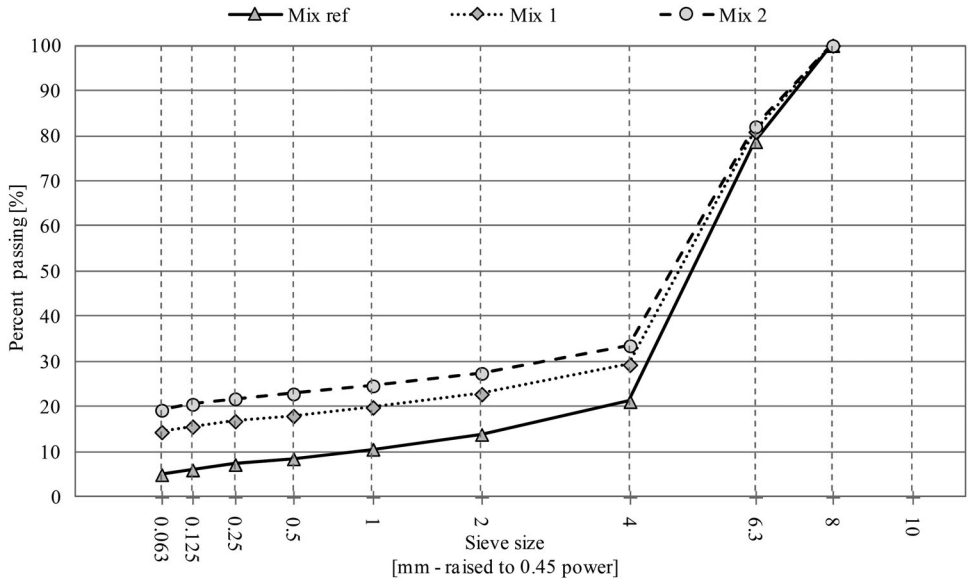

Figure 4. Gradations Mix ref, Mix 1, and Mix 2.

In Mix 1, the amount of extra filler and extra bitumen was added by the following two criteria. The first was to maintain the same D/P of the reference mixture (~1.0). The second was that the volume of the VMA calculated considering the volume of Air Voids (AV), absorbed binder (V_{be}) and extra filler (ΔV_f) was approximately equal to the VMA of the reference mixture. Considering this, the amount of extra binder (ΔP_b) and extra filler (ΔV_f) were calculated by solving the following system of Equations (3) and (4):

$$\begin{cases} \dfrac{P_{f_{ref}} + \Delta P_f}{(P_{be_{ref}} + \Delta P_{be})} \cong 1.0 \\ \dfrac{AV + V_{be_{ref}} + (\Delta V_{be} + \Delta V_f)}{V_{agg} + V_{be} + AV} \cong 35.2\% \end{cases} \quad (3, 4)$$

Where P and V refer to the % weight and % volume of:

- f_{ref} – of particles passing #0.063 (filler) mm sieve in Mix_{ref};
- be_{ref} – effective binder in Mix_{ref};

and where:

- δP_f – %weight extra-filler, ΔV_f – %volume extra-filler;
- δP_{be} – %weight of extra effective bitumen, ΔV_{be} – %volume of extra effective bitumen;
- AV – represents the air voids in the compacted mix [%];
- V_{agg} – represents the volume of aggregates in the mix including the filler [%];
- V_{be} – represents the volume of effective binder in the mix which is equal to $V_{be\ ref}+\Delta V_{be}$ [%];

Equations (3) and (4) were developed in this work to meet the criteria at the base of the design of mixes for damping layers considered in this work. Equation (3) refers to the criteria of the mastic stiffness discussed above. Equation (4) indicates that in Mix 1, the entire VMA has been filled with the rubberised mastic to maximise the damping. The comparison of the VFA of Mix_{ref} (Table 2–23.8%) with those of Mix 1 (Table 3–98.4%), showed that in the latter almost all the VMA available were saturated with the mastic. The volume of mastic in Mix 1 was limited by the VMA of Mix_{ref} to preserve a sufficient level of aggregates interlock.

Mix 2 was prepared by following the same considerations of Mix 1 (Equations (3) and (4)) but an extra amount of binder (5% in weight) was added to go beyond the saturation of the VMA in the Mix_{ref} to increase further the damping of the mixture. In this case, results of Equation (4) showed that the VMA filled with extra-mastic (ΔV_f and ΔV_{be}) is equal to 44.1% with the VFA in the mix equal to 99.6%. The values of the VMA and the VMA filled with extra-mastic (Equation (4)) are given in Table 4.

The behaviour of the mixes under compaction is discussed in Section 4.1.

3.4. Experimental testing

3.4.1. Indirect tensile strength (ITS) and water sensitivity

The test was conducted on 100 mm diameter on SGC compacted samples. Mixing and compaction temperatures were kept at 180°C, and the number of gyrations for each mix is given in Table 2 (Mix_{ref}) and Table 3 (Mix 1 & 2). The samples were tested at two conditions by using three replicates for each condition. The first is the dry condition, which was conducted on dry samples conditioned at 25°C according to EN 12697–23 (2012). The second was the wet condition that was conducted at 25°C on samples conditioned in a water bath at 40°C for 72 h, according to EN 12697–12 (2008).

The Indirect Tensile Strength (ITS) was calculated according to Equation (5).

$$ITS\ [MPa] = \frac{2P}{\pi DH} \quad (5)$$

where:

Table 3. Volumetric properties (by weight – W; and by volume – V) Mix 1 and Mix 2 (EN 12697 – Part 5, 6) (2012).

Mix		Aggregates [%]	Filler [%]	Binder [%]	N_{max} [-]	AV[%]	VMA [%]	VFA [%]	D/P [-]
Mix 1	W	85.3	14.7	14.8	130	-	28.0	98.4	0.99
	V	61.4	10.6	27.6		0.4			
Mix 2	W	80.2	19.8	20.0	130	-	34.2	99.6	0.99
	V	52.8	13.0	34.1		0.1			

- P is the peak load [N];
- D is the sample diameter [mm];
- H is the sample height [mm].

The ITS is measured in dry (ITS_d) and wet (ITS_w) conditions. The ratio between the values at the two conditions was a measure of the moisture susceptibility of the mixture intended as the loss in tensile strength due to the effects of water (Indirect Tensile Strength Ratio – ITSR, Equation (6)).

$$ITSR\ [\%] = \frac{ITS_w}{ITS_d} \times 100 \tag{6}$$

3.4.2. Dynamic modulus |E*| and phase angle(δ)

The viscoelastic properties of the different mixes were measured according to the AASHTO TP 79 (2012) standard. For each mixture, two 150 mm diameter samples were prepared in the SGC. The samples were compacted to a height of 175 mm. After compaction and cooling at room temperature, the samples were cored to a diameter of 100 mm and cut at the height of 150 mm. An example is shown in Figure 5 (a).

Three strain gauges were attached at intervals of 120° considering the cross-section of the sample. The gauge length was 70 mm measured centre-to-centre of the gauge point (Figure 5. Dynamic modulus and phase angle test sample (a), and test set-up (b,c).

- b). Teflon sheets were used at the top and bottom edges of the sample to avoid friction with the loading plates (Figure 5-c). The test conditions are reported in Table 5.

The test temperatures were determined according to standard AASHTO TP 79 and other studies (Yu *et al.* 2013, Zelelew *et al.* 2013). The highest temperature (i.e. 31°C) was selected since it represents the average design pavement-temperature of 31 °C for Tuscany region (Cuciniello *et al.* 2020). It should be noted that a higher test-temperature (e.g. 54°C) was not preferable, since such high temperature may cause the Mix 1 and Mix 2 to deform and cause the test to fail. The selection of the eight loading frequencies was based on the existing literature as well, and they were also recommended in the control-system software of the laboratory equipment.

For the confinement condition, the confined condition test can increase the stiffness of the mixture compared to the unconfined condition (Timm *et al.* 2012, Diefenderfer and Link 2014). Taking into account the lower stiffness of the designed damping mixture, the confined conditions is easier to ensure the completion of the test. However, as the dynamic modulus test specified by Mechanistic Empirical Pavement Design Guide (MEPDG) (Lacroix *et al.* 2011; Willis 2013), the unconfined test was selected in this study, in order to provide input parameters for the subsequent simulation process with MEPDG as the model. At the same time, the simplicity of unconfined testing was another reason to consider (Willis 2013).

Table 4. VMA and $VMA_{with\ extra\text{-}mastic}$ values at N_{max}.

Mixture	VMA	VMAwith extra-mastic Equation (4)
Mix_{ref}	35.2%	-
Mix 1	28.0%	35.2%
Mix 2	34.2%	44.1%

The master curves of the Dynamic Modulus (|E*|) and the phase angle (δ) were developed under the applicability of the time-temperature superposition principle (TTSP) (Ferry, 1980). The horizontal shift factors were calculated by the William-Landel-Ferry (WLF) (Equation (7),

$$\log \alpha_T = -\frac{C_1 \cdot (T - T_{ref})}{C_2 + (T - T_{ref})} \tag{7}$$

where:

- α_T – is the shift factor;
- C_1 and C_2 – are equation parameters;
- T_{ref} – is the reference temperature (i.e. 20°C);
- T – is the testing temperature.

The dynamic modulus (|E*|) and the phase angle data were modelled by using the Modified Christensen-Anderson-Marasteanu (CAM) model (Zeng *et al.* 2001).

The |E*| master curve of the CAM model is given by Equation (8).

$$|E^*|\ [Mpa] = E_e + \frac{E_g - E_e}{\left[1 + \left(\frac{f_c}{f_r}\right)\right]^{\frac{m_e}{k}}} \tag{8}$$

where:

- |E*| – is the dynamic modulus;
- E_e – is the Equilibrium Modulus, which represents the value of stiffness at f→0. Its value represents the horizontal asymptote in the low frequencies region. In the case of mixes, its value is considered to depend on the ultimate aggregate interlock when the contribution of the binder (or the mastic) results negligible.
- E_g – is the Glassy Modulus, which represents the value of stiffness at f→∞. Its value represents the horizontal asymptote in the high frequencies region.
- f_r – is the reduced frequency;
- f_c – it is a location parameter that has the dimension of frequency. It is known as crossover frequency, which is the

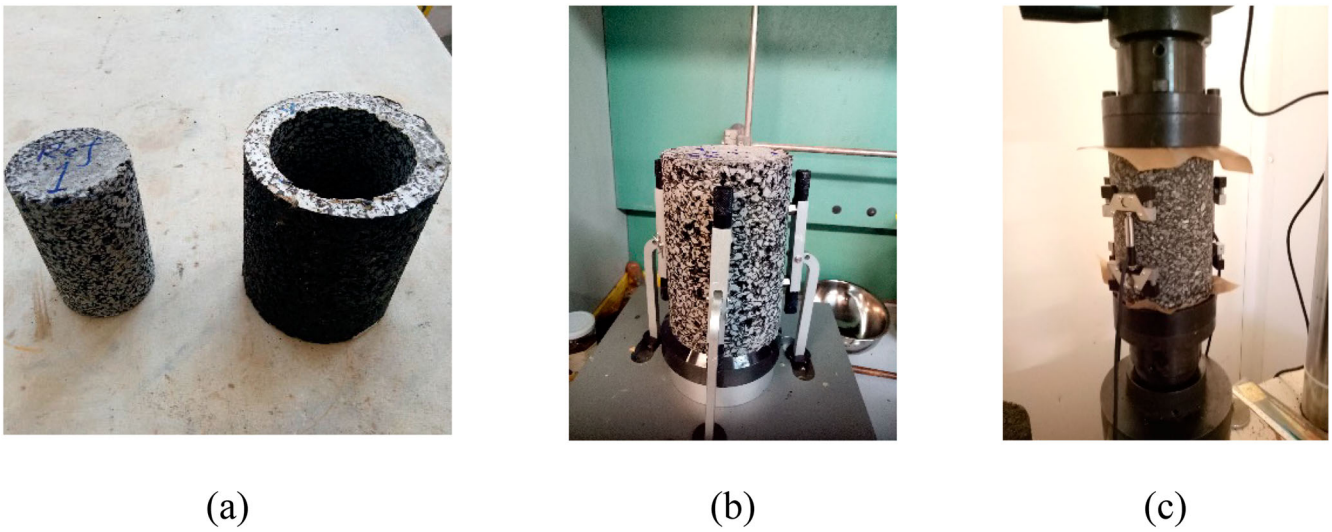

Figure 5. Dynamic modulus and phase angle test sample (a), and test set-up (b,c).

frequency where the storage modulus (E') is equal to the loss modulus (E'').
- m_e, k– dimensionless shape parameters.

The CAM model equation of the phase-angle master curve is given by Equation (9).

$$\delta[^\circ] = 90I - (90I - \delta_m)\left[1 + \left(\frac{\log(f_d/f_r)}{R_d}\right)^2\right]^{-\frac{m_d}{2}} \quad (9)$$

$$\begin{cases} I = 0 & \text{for mixes} \\ I = 0 & \text{if } f_r > f_d \\ I = 1 & \text{if } f_r < f_d \end{cases}$$

where:

- δ – is the phase-angle;
- δ_m – is the phase-angle value at f_d. In the case of mixes, it represents the maximum phase-angle value;
- f_d – it is a location parameter with the dimension of frequency. It is the frequency at which δ_m occurs;
- f_r – is the reduced frequency.

The measure of the phase angle is critical because it represents a measure of the internal damping. High values of phase angle imply high internal friction and therefore, more dissipative behaviour under loading (a more viscous behaviour). On the other side, lower values of phase angle denote a more elastic response of viscoelastic materials, which indicates the higher capacity of storing energy under loading cycles; the master curve of the damping ratio was derived from the phase angle one applying Equation (2).

Table 5. Test conditions for dynamic modulus, phase angle, and damping ratio test.

Test conditions	Configuration
Test temperature [°C]	5, 20, 31
Loading frequency [Hz]	0.1, 0.5, 1, 2, 5, 10, 20, 25
Strain level	100 μs
Confinement	Unconfined conditions

3.4.3. Hamburg wheel tracking (HWT) test

The Hamburg Wheel Tracking test was conducted at wet conditions to evaluate the rutting resistance of mixes and to substantiate the results of the ITSR test on the moisture susceptibility according to AASHTO T 324 (2007). The test temperature was equal to 50°C, and the test was concluded at 10,000 cycles or when the maximum allowable rut depth limit (12.7 mm) was achieved. Four mixture 'configurations' were used in the test (Figure 6) with the specific aim of understanding the rutting resistance of the damping material used as the interlayer. For this reason, the test was arranged in such a way to compare the rutting resistance of the damping material with that of a control mix.

The control mix was a Gap Graded Wet Rubberised Mix (GGW) traditionally used in wearing course layers to optimise friction and acoustic performances (Figure 6(a)), since it will be used in conjunction with the damping mixture (GGW for the surface layer and damping mixture for the damping interlayer), as an integral part of the future overall research. Details on the control mix can be found in the literature (Losa *et al.* 2012).

Mix 1 and Mix 2 were used as interlayers between two slices of the GGW mixture, as shown in Figure 6b and c. These layered samples were prepared directly in the SGC according to the following method (see Figure 7):

- The mixture for the bottom slice was compacted firstly at one gyration to flatten the top surface (①-③);
- Then, the middle slice mixture was introduced in the mould and compacted at one gyration for the same scope (④-⑥).
- Then the top slice mixture was introduced in the mould, and the layered system was compacted to achieve a thickness of 100 mm (48 gyrations) (⑦-⑩).

An image of the longitudinal section of a layered sample is given in Figure 8.

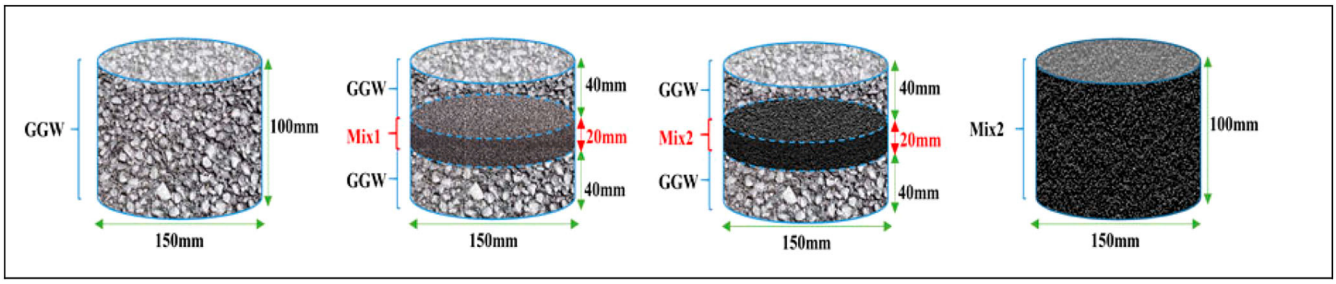

Figure 6. Mixture configurations used in the HWT test. (GGW – Gap Graded Wet Rubberised Mix)

The SGC was used to compact samples to diameter 150 mm and thickness 100 mm. The level of compaction was defined to N_{design} (i.e. 50 gyrations) for all the four mixture configurations.

Results were analysed according to the Texas DOT (TEX-242-F, 2014) by considering the rut depth measured after 10,000 cycles as the test outcome.

4. Results and discussion

4.1. Workability

The design of the mixes has been well detailed in §3.2. The volumetrics have been discussed to provide the main concepts behind the design methodology adopted (Table 3). In this section, some considerations on the compactability of mixes have been included by referring to the compaction curves from the SGC (Figure 9), and to the volumetrics at N_{ini}, N_{des} and N_{max} that are given in Table 6.

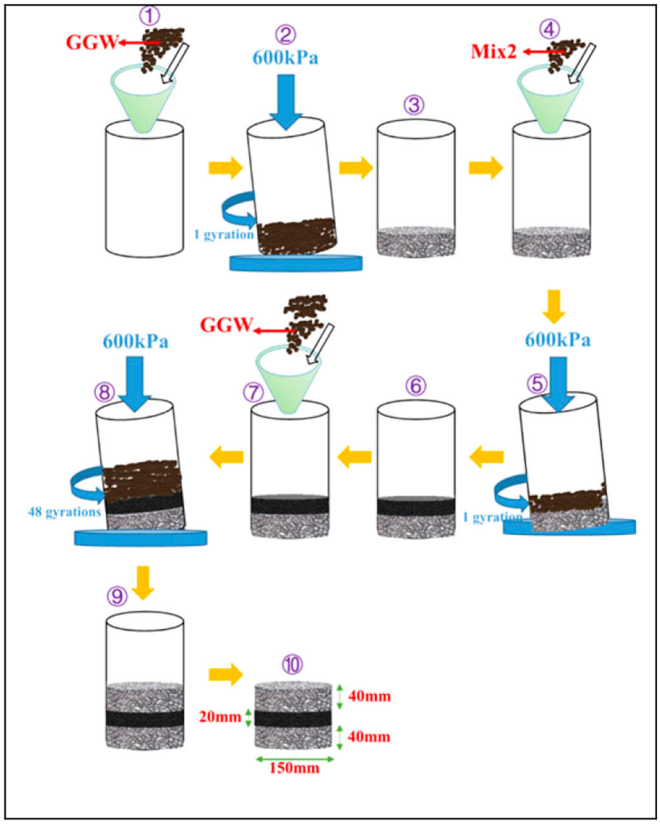

Figure 7. Preparation of layered samples for HWT test

The reference mixture showed the behaviour of a typical OG mixture maintaining a level of air voids above 25% even after the maximum compaction effort provided (i.e. 130 gyrations). The variation in the volumetrics of Mix 1 and Mix 2 depended on the higher volume of binder in the mix (Table 3). If Mix_{ref} was prepared with the 5.0% asphalt content as the percentage of the mass of aggregates, Mix 1 included about three-times this value (14.8%), while Mix 2 about four-times (20.0%). The first (Mix1) showed a volume of air void below 10% already at the beginning of compaction to achieve about 0.5% air voids at N_{max}; in the second (Mix2), the variation in the air voids under the compaction effort appears quite narrow (1.2%) due to the extra amount of binder (and filler) included for maximising damping. It is understood that in this case, the volume of air voids below 1.0% at N_{max} could raise concerns of rutting resistance and bleeding. However, such an unconventional mixture was not considered for wearing course layer. Besides this, rutting resistance was carefully investigated through the HWT. For this reason, the analysis of the compactability of the two mixes does not highlight critical shortcomings. Additionally, Mix 1 has been used in a field test section conducted in Prato (Italy) in 2019, showing no problem with workability of the mixture during mixing, paving and compaction processes.

4.2. Indirect tensile strength (ITS) and water sensitivity (ITSR)

Results of the ITS test conducted on dry and wet-conditioned samples are given in Table 7. The replicates for each mix and test were used.

The ITS and ITSR values of the mixes were compliant with the specification at both, the dry and the wet conditions. The reduction in the ITS_{dry} values of Mix 1 and Mix 2 compared with Mix_{ref} can be attributed to the high volume of bitumen, which can reduce the aggregate interlock affecting the tensile strength.

On the other hand, a higher amount of binder (and filler) tends to increase the thickness of the mastic film coating the aggregates; this results in higher ITSR values of Mix 1 and Mix 2 in comparison with Mix_{ref}. Besides this, a more than adequate resistance depended on the use of CRMB, whose reduced moisture susceptibility has

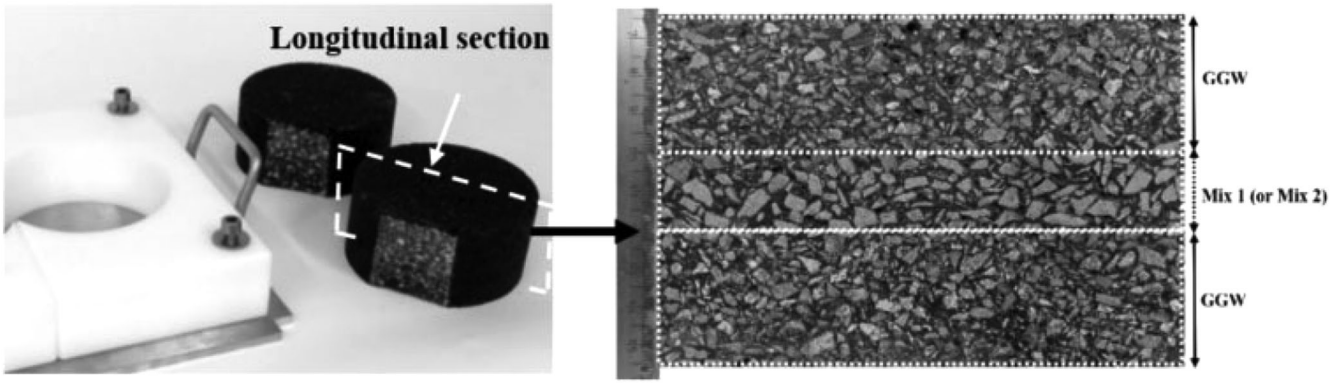

Figure 8. Longitudinal Section of HWT layered samples (GGW + Mix 1 and GGW + Mix 2).

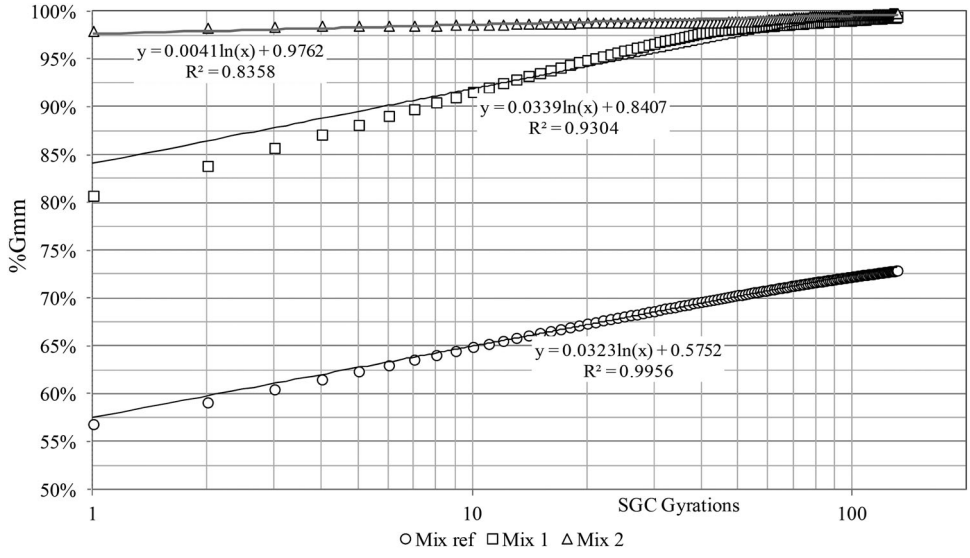

Figure 9. Compaction curves of mixes prepared with samples of 150 mm.

been proven by several studies (Leandri *et al.* 2014, Sangiorgi *et al.* 2017).

4.3. Dynamic modulus (|E*|) and phase angle (δ)

The master curves of the dynamic modulus (|E*|) and the phase angle (δ) of the mixes are given in Figures 10 and 11.

The master curves were developed on two replicates. Results show an acceptable variability, with the coefficient of variation of the average between two samples below 10% for all the cases. The shift factors were optimised on the dynamic modulus master curve and were then applied to the phase angle master curve. The CAM model provides an adequate accuracy in modelling the raw data with the R^2 coefficient being above 97% (for modulus) and 95% (for phase angle) for all mixes.

The reference mixture shows the highest levels of stiffness (Figure 10) and the lowest values of phase angle (Figure 11) in the range of reduced frequency considered. This aspect was expected due to the differences in the composition between the mixes. The higher stiffness of the OG mixture is in agreement with the tensile strength values (Table 7) and depends on the higher aggregate interlock provided by a thinner film of mastic. The difference between Mix_{ref} and the two damping mixes is well visible in the low-frequencies region where the aggregate structure is more significant than the mastic. The difference between the horizontal asymptotes in this region is of multiple orders of magnitudes.

Mix 1 and Mix 2 show similar levels of stiffness in the intermediate and low range of frequencies, with Mix 1 becoming stiffer at lower temperatures (higher frequencies) and Mix 2 stiffer at higher temperatures (lower reduced frequencies). In addition, it can be observed at the very low range of reduced frequencies (10^{-10} Hz ~ 10^{-6} Hz), the stiffness values of Mix 1 and Mix 2 tend to be very similar. This may be explained by the fact that asphalt tends to be viscous and the stiffness reflects more of the aggregate structure's ability to resist deformation under load. According to Figure 4, Mix 1 and Mix 2 have similar aggregate gradation (and thus structure), so they can exhibit same stiffness moduli under such loading condition. However, such consideration, although plausible, needs to be considered as a hypothesis since the trend of the master curve within this reduced frequency is purely calculated from the model.

Table 6. Volumetric of mixes.

	$N_{-gyrations}$	G_{mm} [kg/m^3]	G_{mb} [kg/m^3]	VA [%]	VMA [%]	VFA [%]
Mix_{ref}	N_{ini}=10	2.520	1.645	34.7	42.3	17.8
	N_{des}=50		1.774	29.6	37.7	21.5
	N_{max}=130		1.838	27.0	35.5	23.7
Mix 1	N_{ini}=10	2.249	2.071	7.9	33.6	76.4
	N_{des}=50		2.211	1.7	29.1	94.2
	N_{max}=130		2.238	0.5	28.2	98.2
Mix 2	N_{ini}=10	2.143	2.114	1.3	35.2	96.2
	N_{des}=50		2.121	1.0	35.0	97.1
	N_{max}=130		2.140	0.1	34.4	99.6

Table 7. ITS test results.

Mixes	ITS_{dry}[MPa]	ITSR [%]	ITS_{dry}@25°C[MPa]*	ITSR [%]*
Mix ref	0.62 (±0.04)	82.3	≥0.4	≥80
Mix 1	0.55 (±0.03)	87.3		
Mix 2	0.41 (±0.01)	87.8		

On the other hand, at the very high range of reduced frequencies (>10^2 Hz), the dynamic modulus of Mix 1 is sensibly higher than Mix 2. This may be due to the higher content of mastic in Mix 2, which lowers the stiffness of the mixture.

The shape of the δ master curves was typical of mixes (Figure 11). At the very low reduced frequency, as mentioned above, mixtures' behaviour was dominated by the aggregate properties rather than asphalt binder. This implies that the phase angle and reduced frequency were correlated (i.e. as reduced frequency increases phase angle increases as well). However, at high reduced frequency, the mixtures' behaviour was mostly dominated by asphalt binder properties. For a viscoelastic material like asphalt binder, reduced frequency, and phase angle are negatively correlated. While at the intermediate region, the response is controlled by both the constituents (aggregate and binder) showing visible viscoelastic behaviour. Peak of the phase angle master curve corresponds to the transitioning phase, where mixtures' behaviour transitions from being more dominated by the binder (or mastic) to the aggregate skeleton. With respect to the binder content on the phase angle, the maximum phase angle slightly shifts to the left with the decrease of the binder content (Mix 2 to Mix 1). Such a change is expected because at the intermediate and high reduced frequency, decrease of rubberised binder can cause a decreases in the phase angle, and an increase in the stiffness and elasticity. As a result, asphalt mixture is able to remain in the more binder-dominated phase for a longer range of reduced frequency, and to transition to the more aggregate-dominated phase at a slower reduced frequency.

The values of the phase angle support what was the main scope of the mix design that is, increasing the damping response of mixes – Mix 1 and Mix 2 show consistently higher phase angle values than the reference mixture. Higher phase angle values indicate a more viscous response under loading with a consequent higher energy dissipation and reduction of the vibratory mechanism. Although the phase angle is representative of the damping properties, the comparison between the damping properties of mixes is given in the next section in terms of the damping ratio.

4.4. Damping properties

The damping ratio master curve is given in Figure 12.

The damping ratio values were calculated from the phase angle values using Equation (2). Therefore, the master curves of the two viscoelastic functions have similar trends. At low frequencies, the aggregate skeleton has a stronger influence on the response, which is more elastic; for this reason, ζ decreases. At the very high frequencies, the mastic becomes stiffer and more elastic, lowering ζ again. In the intermediate region, the response is controlled by both the aggregate skeleton and the mastic showing a visible time dependency (viscoelasticity). In this region, the peak is likely to represent the threshold between the effects of the two constituents. On the right side of the peak, the mastic phase controls more the response. On the left side, vice versa. Mix 2 shows the peak at higher frequencies than Mix 1 and Mix_{ref}. In this case, the higher amount of binder makes the mixture more

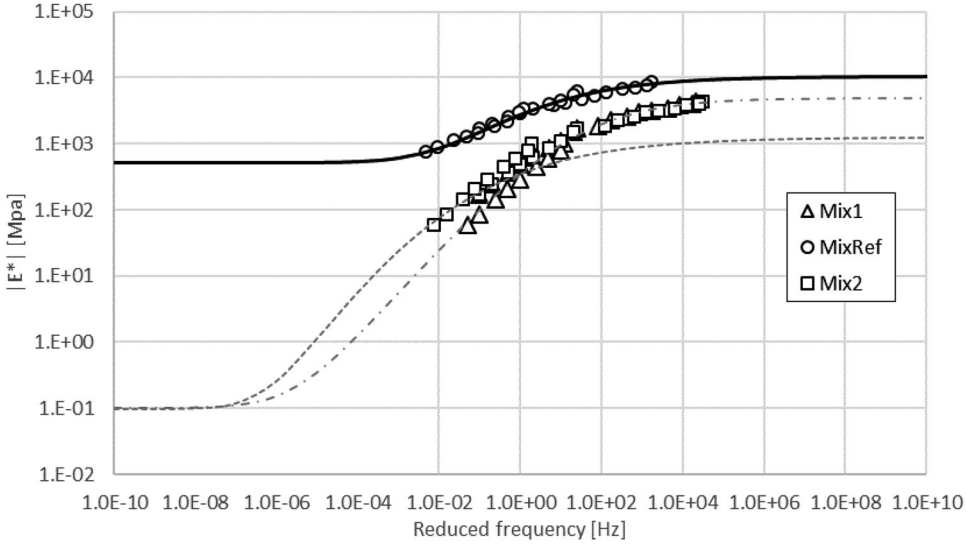

Figure 10. Dynamic modulus master curves.

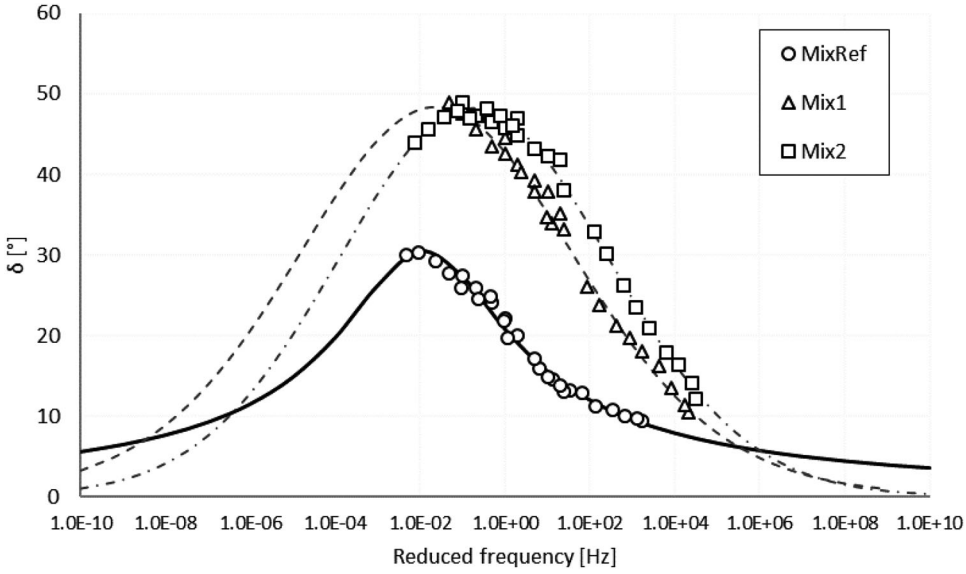

Figure 11. Phase angle master curves.

temperature-susceptible and moves the peak towards higher frequencies (or lower temperatures). In other words, Mix 2 shows higher damping at lower temperatures. However, irrespective of frequency, Mix 1 and Mix 2 display consistently higher values of damping ratio than Mix_{ref}, showing a better capacity for mitigating the vibration mechanism. In addition, Mix 1 and Mix 2 with maximum damping ratio of 0.6 show nearly twice value of Mix Ref, indicating the damping characteristics of Mix 1 and Mix 2. However, in practical damping applications used in the pavement, utility over wide ranges of temperature and frequencies is also required (Guanjun 2012, Beniah *et al.* 2016). Thus, high damping ratio values over a broad temperature and frequency window are desired good damping performance. Also, different from traditional damping materials, asphalt mixture not only requires high energy dissipation capacity, it also needs to have a certain load-bearing as the composition of the road structure layer. In other words, the higher stiffness in the high damping range is more desired (Guanjun 2012). Table 8 summarises the damping characteristics of the three asphalt mixtures under a broader evaluation index at 20°C. ζ_{max} represents the maximum damping ratio; f @ ζ_{max} represents the reduced frequency related to ζ_{max}; f @ $(\zeta_{0.7})$ corresponds to a 3 dB drop from the peak of the damping ratio (Umashankar *et al.* 2009, Guanjun 2012), in other words, it represents the corresponding frequency range when the damping ratio is higher than 70% of ζ_{max}; f @ $(\zeta_{>0.15})$ corresponds the frequency range when the damping ratio is higher than 0.15, which represents the effective damping ratio for the conventional damping materials.

For the three mixes, all values of $f@\zeta_{max}$ are included in the range of typical values of traffic load frequency, indicating that it is practical for asphalt mix to achieve the maximum vibration absorption capacity under traffic load. In addition, it is evident that Mix 1 and Mix 2 include a wider frequency range to obtain the effective damping, regardless of $f@(\zeta 0.7)$

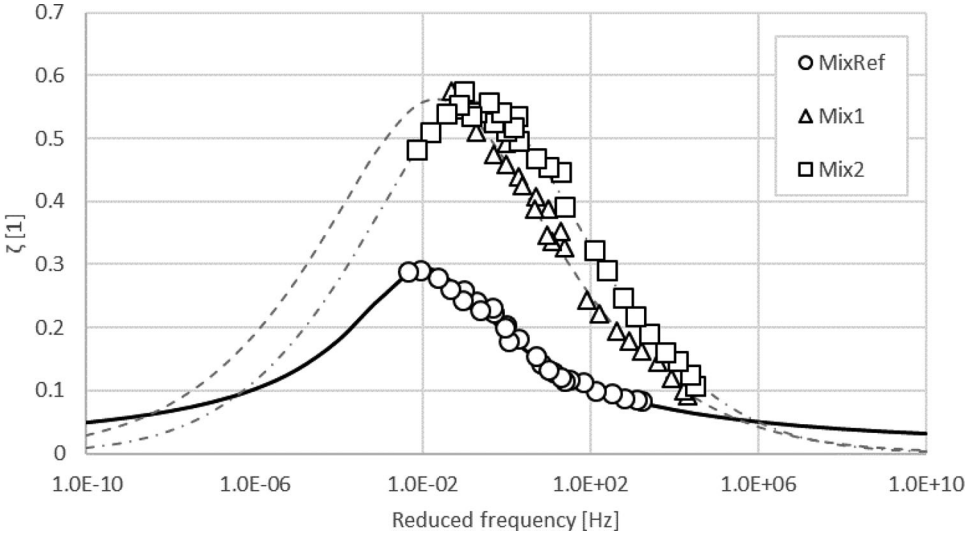

Figure 12. Damping ratio master curves.

Table 8. HWT test results (average values on two couple of specimens).

Parameters	UoM	GGW	GGW-Mix 1	GGW_Mix 2	Mix 2
Creep Slope (x1000)	mm/cycles	0.0563	0.0426	0.0506	0.4000
Strip Slope (x1000)	mm/cycles	-	-	-	-
# cycles @ 12.7 mm	cycles	> 10,000	> 10,000	> 10,000	247
Rut depth @ 10,000 cycles	mm	3.1	2.2	2.1	12.7

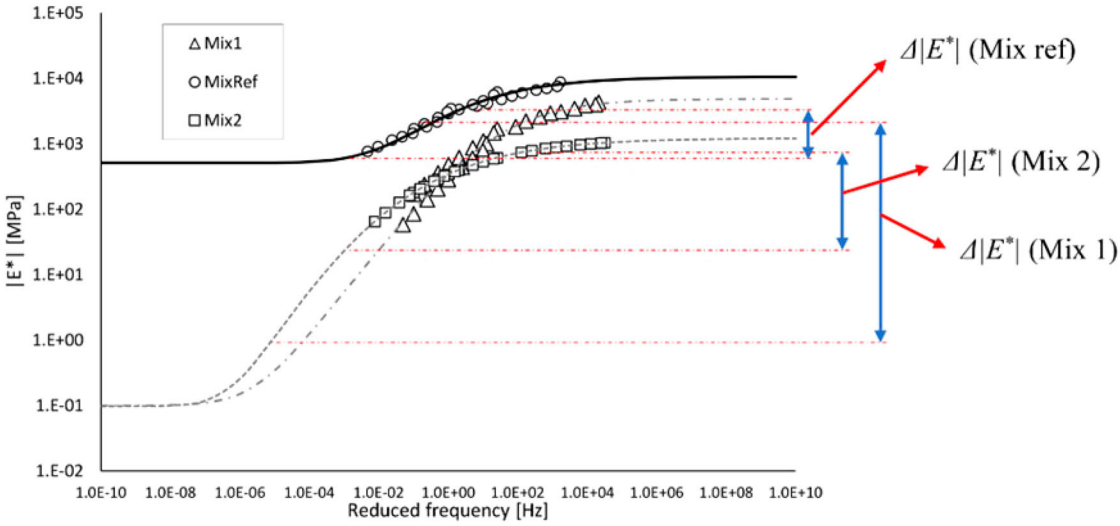

Figure 13. |E*| as the damping ratios are higher than 70% of ζ_{max}.

or *f@(ζ>0.15)*. Moreover, such frequency range is closer to the actual traffic load. Comparing with Mix 1, Mix 2 showed more obvious damping effect for higher loading frequencies.

Figure 13 shows the results of |E*| as the damping ratios are higher than 70% of ζ_{max}. It is evident Mix ref shows higher stiffness within the effective damping range, which is beneficial to improve the stability of pavement. Compared with Mix1, the stiffness of Mix 2 in the effective damping range is mostly at a higher level. However, for Mix1 under low-frequency load, in order to obtain a high damping ratio, it is forced to reduce the stiffness. Hence, from this perspective, Mix 2 is more desired.

In the design of mixtures for damping layers, the damping ratio should be quantitatively determined as a key-factor controlling the vibratory mechanism. However, ζ may not be representative of the structural damping of the pavement because the latter is exposed to the external factor and boundary conditions that affect the vibratory mechanism and cannot be accounted for the material damping. Findings of Huang (2019), show that to provide an adequate reduction of pavement vibration, the material-damping ratio (of a damping layer) should be at least twice that of a conventional asphalt mix. As can be seen from Figure 12, the mixtures designed as a damping layer (i.e. Mix 1 and Mix 2) meet this requirement within a wide interval of reduced frequencies, ranging from 10^{-2} to 10^{2} Hz, which covers the typical values of traffic loading frequencies (Losa and Di Natale 2012).

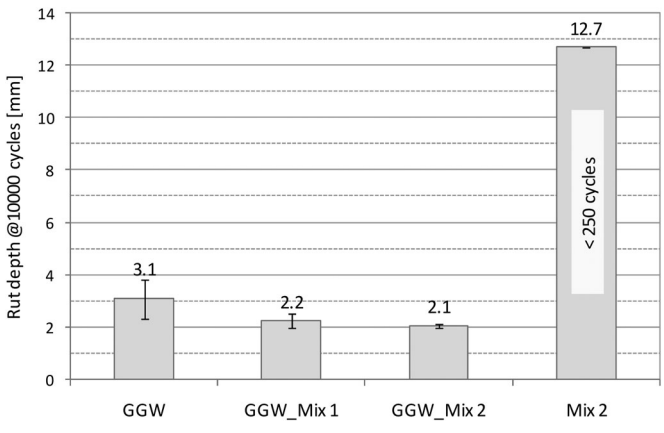

Figure 14. Hamburg Wheel Test results: rut depth after 10,000 cycles.

4.5. Hamburg wheel tracking (HWT) test

The results of the HWT test are given in Figure 14 and Table 8.

In the case of the Mix 2 test was interrupted after 250 cycles since the rut depth was higher than 12.7 mm already within this number of cycles. The rutting susceptibility of Mix 2 was also observed during compaction (§4.1).

Before discussing the other mixes, it is worth recalling that Mix 1 and Mix 2 are meant to be used as interlayers. Therefore, their rutting resistance has been evaluated with them being used as an interlayer in a layered sample (Figure 6). The layered nature of the samples of the HWT test was indicated by their labels (Figure 14 – GGW_Mix 1 (GGW + Mix 1 + GGW) and GGW_Mix 2 (GGW + Mix 2 + GGW)).

The final rut depths of the layered mixes are similar and are lower than the one of a traditional Gap Graded mixture prepared with the rubberised binder (wet method – GGW)

(Figure 14). This aspect indicates that the use of Mix 1 and Mix 2 as an interlayer does not worsen the rutting resistance of the whole sample, but contrarily, it provides a beneficial effect. The higher rutting resistance of the layered mixes is confirmed by the values of the creep slope in Table 8.

This result can be explained as follows. The GGW mix incorporates a volume of voids approximately 5%. For this reason, part of the volume of such a mixture is prone to reduce under the effect of the loading wheel (densification). On the other hand, when an important part of the bulk volume is occupied by a region where the air volume is around 2% or below (i.e. Mix 1 and Mix 2), the densification (and shear failure) is less prone to occur.

Concerning the moisture susceptibility, results from the HWT confirm the results of the ITSR (§4.2) with the mixes that do not show stripping during the test.

5. Conclusions and future development

5.1. Conclusions

This paper proposes the basis for the development of a design method of damping mixes that aim at reducing traffic-induced vibration. The method is based on the concept that high volumes of rubberised binder (wet method) in asphalt mixes increase their damping response, decreasing the vibratory mechanism under dynamic loading. Results of mix design allow raising the following conclusions and considerations:

- As one of the key objectives in the present study, a mix design method specifically adapted to the damping layer is innovatively proposed, and the specific technical means for its implementation are summarised as follows. Using an Open Graded (OG) mixture as a starting point provides a sufficient VMA to accommodate the largest amount of binder (mastic) to increasing damping while maintaining an adequate aggregate structure. The binder content should be increased by maintaining the same dust proportion (D/P) to prevent the mastic phase from softening with a consequent loss in stability and stiffness of the mixture. In this sense, the VMA of the OG mixes have been filled with rubberised asphalt and filler by maintaining almost constant the D/P – Mix 1 was prepared with 14.8%(w/w) of binder, while Mix 2 with 20.0% (w/w) of the binder.
- Findings from mechanical characterisation highlight that:
  - The mixes for damping layers show a sensibly lower volume of voids due to the completely filling of mastic. The massive amount of bitumen in Mix 2 caused the voids of the mix collapsing already at the beginning of compaction. However, the designed mixes do not show problems during compaction.
  - Despite the increase in bitumen content, the indirect tensile strength of Mix 1 and Mix 2 complies with current specifications for OG mixes. Besides this, the use of higher volumes of rubberised binder reduces the moisture susceptibility of the mixes compared to the reference one. This result can be confirmed by other works.
  - The high levels of binder used in Mix 1 and Mix 2 contribute to decreasing the stiffness compared to the reference mixture. Such a softening is well visible in the range of low frequencies were the level of interlock in the aggregate skeleton is reduced by the thicker film mastic. In the range of intermediate and high frequencies, Mix 1 and Mix 2 have comparable levels of stiffness, with the latter becoming stiffer at higher frequencies.
  - The phase-angle master curves show a typical trend of mixes characterised by the presence of a peak. Mix 1 and Mix 2 show higher values of phase angle in the whole frequency interval, therefore they provide a more viscous response under dynamic loading. Decrease of rubberised binder/mastic can remain asphalt mixture in the binder-dominated phase for a longer range of reduced frequency, and to transition to the aggregate-dominated phase at a slower reduced frequency. Mix 1 and Mix 2 display consistently higher values of damping ratio than Mix ref, showing a better capacity of mitigating the vibration mechanism.
  - Rutting was one of the major concerns for the design of such mixes. However, results from the HWT have shown that the use of Mix 1 and Mix 2 as an interlayer in a Gap Graded Mixture does not affect the rutting resistance of the layered mixture.
- The functional properties of the designed mixture were tested by the damping ratio. Mix 1 and Mix 2 show higher damping than the reference mixture in the whole range of frequencies. The higher capacity of dissipating energy under loading reflects a higher ability to dissipate the vibratory mechanism. Due to the larger binder content, Mix 2 shows a higher temperature susceptibility and provides the highest level of damping at a lower temperature than Mix 1 and Mix_{ref}. Compared to Mix ref, both Mix 1 and Mix 2 can include a wider frequency range to obtain the effective damping, while considering higher stiffness in the low-frequency range, Mix 2 is more desired. The designed mixture can meet the requirements of damping ability under typical traffic loading frequencies.

5.2. Future development

The research results at this stage, including the design of the mixture, the characterisation of mechanical and functional characteristics, were sufficient to prove the feasibility of the designed mixture used in the damping layer. The next stage of the development process will focus on the use of Mix 1 and Mix 2 for field tests of road structures with damping layers, which will be introduced in the followed-up studies.

Disclosure statement

No potential conflict of interest was reported by the author(s).

ORCID

Giacomo Cuciniello http://orcid.org/0000-0002-8111-5672

References

American Association of State Highway and Transportation Officials, 2007. *AASHTO t 324-04. Standard test method for Hamburg wheel*

track testing of compacted hot-mix Asphalt (HMA). Washington, DC: AASHTO.

American Association of State Highway and Transportation Officials, 2012. *AASHTO TP 79. Method of test for determining the dynamic modulus and flow number for asphalt mixtures using the asphalt mixture performance tester (AMPT)*. Washington, DC: AASHTO.

America Society for Testing Materials, 2002. *ASTM D6114-97 (Version 2002). Standard specification for asphalt-rubber binder*. Philadelphia: astm.

Bahia, H.U., *et al.*, 2001. Characterisation of modified asphalt binders in Superpave mix design (NCHRP Project 9-10).

Beniah, G., *et al.*, 2016. Novel thermoplastic polyhydroxyurethane elastomers as effective damping materials over broad temperature ranges. *European Polymer Journal*, 84, 770–783.

Bergman, L.A. and Hannibal, A.J., 1976. An alternate approach to modal damping as applied to seismic-sensitive equipment. *The Shock and Vibration Bulletin*, 46 (Part II), 69–82.

Biligiri, K.P., 2013. Effect of pavement materials' damping properties on tyre/road noise characteristics. *Construction and Building Materials*, 49, 223–232.

Browne, M., *et al.*, 2012. Reducing social and environmental impacts of urban freight transport: a review of some major cities. *Procedia - Social and Behavioral Sciences*, 39, 19–33.

Cantisani, G., Fascinelli, G., and Loprencipe, G., 2013. Urban road noise: the contribution of pavement discontinuities. *In*: *Icsdec 2012: developing the frontier of sustainable design, engineering, and construction*, 327–334.

Cho, Y.H., *et al.*, 1998. *Asphalt overlay design methods for rigid pavements considering rutting, reflection cracking, and fatigue cracking*. University of Texas at Austin. Center for Transportation Research, No. TX-98/987-9.

Christensen, D.W. and Bonaquist, R.F., 2005. VMA: One key to mixture performance. *National Superpave News*, 4 (3), 6–7.

Clemente, P. and Rinaldis, D., 1998. Protection of a monumental building against traffic-induced vibrations. *Soil Dynamics and Earthquake Engineering*, 17 (5), 289–296.

County, S., 1999. *Report on the status of rubberised asphalt traffic noise reduction in Sacramento County*. Sacramento County: Bollard & Brennan Inc.

Cuciniello, G., *et al.*, 2020. Effects of ageing on the damage tolerance of polymer modified bitumens investigated through the LAS test and fluorescence microscopy. *International Journal of Pavement Engineering*, 51, 1–12.

Diefenderfer, B.K. and Link, S.D., 2014. In temperature and confinement effects on the stiffness of a cold central-plant recycled mixture. *Proceedings of the 12th international society for asphalt pavements conference on Asphalt pavements*.

Di Mino, G., *et al.*, 2012. A dynamic model of ballasted rail track with bituminous sub-ballast layer. *Procedia - Social and Behavioral Sciences*, 53, 366–378.

Dondi, G. and Simone, A., 2005. Soluzioni tecniche innovative per la mitigazione del rumore e delle vibrazioni da traffico stradale. *Atti della Conferenza Nazionale sulla politica energetica in Italia.–Università di Bologna–18-19 Aprile*.

Dos Reis, H.L., Habboub, A.K., and Carpenter, S.H., 1999. Nondestructive evaluation of complex moduli in asphalt concrete with an energy approach. *Transportation Research Record: Journal of the Transportation Research Board*, 1681 (1), 170–178.

EN, B., 2008. *12697-12: 2008. Bituminous mixtures – test methods for hot mix asphalt–part 12: determination of the water sensitivity of bituminous specimens*. London, UK: British Standard, BSI.

Feriani, A., and Perotti, F., 1996. The formation of viscous damping matrices for the dynamic analysis of MDOF systems. *Earthquake Engineering & Structural Dynamics*, 25 (7), 689–709.

Ferry, J.D., eds. 1980. *Viscoelastic properties of polymers*. Toronto: John Willey & Sons.

Grandi, F., 2008. *La progettazione di pavimentazioni antivibranti*. Bologna: alma.

Guanjun, C., 2012. *Viscoelastic damping material*. Beijing: National Defence Industrial Press.

Gudmarsson, A., Rydén, N., and Birgisson, B., 2013. Nondestructive evaluation of the complex modulus master curve of asphalt concrete specimens. In *AIP Conference Proceedings* Vol. 1511, No. 1, pp. 1301–1308. AIP.

Hanazato, T., *et al.*, 1991. Three-dimensional analysis of traffic-induced ground vibrations. *Journal of Geotechnical Engineering*, 117 (8), 1133–1151.

Hao, H., Ang, T.C., and Shen, J., 2001. Building vibration to traffic-induced ground motion. *Building and Environment*, 36 (3), 321–336.

Houghton, J.C., 1994. Royal commission on environmental pollution. Eighteenth report. *Transport and the Environment*.

Huang, J., 2019. *Rubber modified asphalt pavement layer for noise and vibration absorption*. Thesis (PhD). University of Pisa.

Huang, J., Losa, M., and Leandri, P., 2018. Determining the effect of damping layers in flexible pavementson traffic induced vibrations. *In*: *Advances in materials and pavement performance prediction – procedings of the international AM3P conference*, Qatar: CRC Press, 255–259.

Hunaidi, O., Guan, W., and Nicks, J., 2000. Building vibrations and dynamic pavement loads induced by transit buses. *Soil Dynamics and Earthquake Engineering*, 19 (6), 435–453.

Hunaidi, O. and Tremblay, M., 1997. Traffic-induced building vibrations in Montréal. *Canadian Journal of Civil Engineering*, 24 (5), 736–753.

Inaudi, J.A., and Kelly, J.M., 1995. Linear hysteretic damping and the Hilbert transform. *Journal of Engineering Mechanics*, 121 (5), 626–632.

Ju, S.H., and Ni, S.H., 2007. Determining Rayleigh damping parameters of soils for finite element analysis. *International Journal for Numerical and Analytical Methods in Geomechanics*, 31 (10), 1239–1255.

Kandhal, P.S. and Chakraborty, S., 1996. Effect of asphalt film thickness on short-and long-term aging of asphalt paving mixtures. *Transportation Research Record: Journal of the Transportation Research Board*, 1535 (1), 83–90.

Kuo, C.M. and Tsai, T.Y., 2014. Significance of subgrade damping on structural evaluation of pavements. *Road Materials and Pavement Design*, 15 (2), 455–464.

Lacroix, A., Underwood, B.S., and Kim, Y.R., 2011. Reduced testing protocol for measuring the confined dynamic modulus of asphalt mixtures. *Transportation Research Record: Journal of the Transportation Research Board*, 2210, 20–29.

Lakes, R., eds. 2009. *Viscoelastic materials*. Bologna: Cambridge University Press.

Lazan, B.J., 1968. *Damping of materials and members in structural mechanics*. Oxford, England: Pergamon Press Ltd. 317.

Leandri, P., Rocchio, P., and Losa, M., 2014. Identification of the more suitable warm mix additives for crumb rubber modified binders. *In*: *Sustainability, eco-efficiency, and conservation in transportation infrastructure asset management*. Pisa: CRC Press, 111.

Losa, M. and Di Natale, A., 2012. Evaluation of representative loading frequency for linear elastic analysis of asphalt pavements. *Transportation Research Record: Journal of the Transportation Research Board*, 2305 (1), 150–161.

Losa, M. and Leandri, P., 2012. A comprehensive model to predict acoustic absorption factor of porous mixes. *Materials and Structures*, 45 (6), 923–940.

Losa, M., Leandri, P., and Cerchiai, M., 2012. Improvement of pavement sustainability by the use of crumb rubber modified asphalt concrete for wearing courses. *International Journal of Pavement Research and Technology*, 5 (6), 395.

Maggiore, C, *et al.*, 2012. Mechanical characterisation of dry asphalt rubber concrete for base layers by means of the four bending points tests. *In*: *3rd four point bending beam conference*. Balkema: CRC Press, 123–138.

Michaels, P., 2008. Water, inertial damping, and the complex shear modulus. *In*: *Geotechnical earthquake engineering and soil dynamics IV*, 1–10.

Nashif, A.D., Jones, D.I., and Henderson, J.P., 1985. *Vibration damping*. John Wiley & Sons.

Ouis, D., 2001. Annoyance from road traffic noise: a review. *Journal of Environmental Psychology*, 21 (1), 101–120.

Paje, S.E., *et al.*, 2010. Acoustic field evaluation of asphalt mixtures with crumb rubber. *Applied Acoustics*, 71 (6), 578–582.

Phillips, C. and Hashash, Y.M., 2008. A simplified constitutive model to simultaneously match modulus reduction and damping soil curves for nonlinear site response analysis. *In*: *Geotechnical earthquake engineering and soil dynamics IV*, 1–10.

Sandberg, U., 1999. Low noise road surfaces-a state-of-the-art review. *Journal of the Acoustical Society of Japan (E)*, 20 (1), 1–17.

Sangiorgi, C., *et al.*, 2017. A complete laboratory assessment of crumb rubber porous asphalt. *Construction and Building Materials*, 132, 500–507.

Schubert, S., *et al.*, 2010. Influence of asphalt pavement on damping ratio and resonance frequencies of timber bridges. *Engineering Structures*, 32 (10), 3122–3129.

Simone, A., Lantieri, C., and Vignali, V., 2008. Vibrazioni da traffico in aree urbane: Effetti sugli edifici e tecniche di attenuazione. *Atti del XVII Convegno Nazionale SIIV–Le reti di trasporto urbano, progettazione, costruzione, gestione-Enna*.

Texas Department of Transportation (TexDOT), 2014. Tex-242-F. *Test procedure for hamburg wheel-trackingtest*. Available from: https://ftp.dot.state.tx.us/pub/txdot-info/cst/TMS/200-F_series/archives/242-0609.pdf. [Accessed October 2019.

Timm, D.H., *et al.*, 2012. *Field and laboratory study of high-polymer mixtures at the ncat test track interim report*. Auburn: National Center for Asphalt Technology, Auburn University.

Umashankar, K.S., *et al.*, 2009. Damping behaviour of cast and sintered aluminium. *ARPN Journal of Engineering and Applied Sciences*, 4, 66–71.

Underwood, B.S., and Kim, Y.R., 2011. Experimental investigation into the multiscale behaviour of asphalt concrete. *International Journal of Pavement Engineering*, 12 (4), 357–370.

UNI, E., 12697-31, 2019. Bituminous mixtures-Test methods for hot mix asphalt-Part, 10.

Venturini, L, Giannattasio, F, and Sangalli, L, 2016. *Anti-vibration pavement: case of study novara municipality*. Novara.

Wang, W. and Höeg, K, 2010. Cyclic behavior of asphalt concrete used as impervious core in embankment dams. *Journal of Geotechnical and Geoenvironmental Engineering*, 137 (5), 536–544.

Wang, Z.Y., Mei, G.X., and Yu, X.B., 2011. Dynamic shear modulus and damping ratio of waste granular rubber and cement soil mixtures. *In*: *Advanced materials research*. Trans Tech Publications, 243, 2091–2094.

Willis, J.R, 2013. Use of ground tire rubber in a dense-graded asphalt mixture on us 231 in alabama: A case study. *In*: *Airfield and highway pavement 2013: Sustainable and efficient pavements*, 1192–1201.

Witczak, M.W., 2002. *Simple performance test for superpave mix design (Vol. 465)*. Washington, DC: Transportation Research Board.

Yu, H. and Shen, S.A,, 2013. Micromechanical based three-dimensional dem approach to characterize the complex modulus of asphalt mixtures. *Construction and Building Materials*, 38, 1089–1096.

Zelelew, H., *et al.*, 2013. Laboratory evaluation of the mechanical properties of plant-produced warm-mix asphalt mixtures. *Road Materials and Pavement Design*, 14, 49–70.

Zeng, M., *et al.*, 2001. Rheological modeling of modified asphalt binders and mixtures (with discussion). *Journal of the Association of Asphalt Paving Technologists*, 70.

Zhong, X.G., Zeng, X., and Rose, J.G, 2002. Shear modulus and damping ratio of rubber-modified asphalt mixes and unsaturated subgrade soils. *Journal of Materials in Civil Engineering*, 14 (6), 496–502.

Zhu, H., and Carlson, D.D., 2001. A spray based crumb rubber technology in highway noise reduction application. *Journal of Solid Waste Technology and Management*, 27 (1), 27–32.

Zinoviev, P.A. and Ermakov, Y.N., 1994. *Energy dissipation in composite materials*. CRC Press.